Journal of Hazardous Materials 161 (2009) 49–54

Contents lists available at ScienceDirect

Journal of Hazardous Materials

journal homepage: www.elsevier.com/locate/jhazmat

Synthesis, characterization, and photocatalytic activities of titanate nanotubes surface-decorated by zinc oxide nanoparticles

Li Shi Wang[a,*], Ming Wei Xiao[b], Xin Jian Huang[a], Yan Dan Wu[b]

[a] College of Chemical Science, South China University of Technology, Guangzhou 510640, PR China
[b] College of Environmental Science and Engineering, South China University of Technology, Guangzhou 510640, PR China

ARTICLE INFO

Article history:
Received 3 January 2008
Received in revised form 11 March 2008
Accepted 11 March 2008
Available online 22 March 2008

Keywords:
Titanate nanotube
Zinc oxide
Photocatalysis
Recycle use

ABSTRACT

Nanoscaled zinc oxide (ZnO) particles with different amounts are coated on titanate nanotubes (TNTs) by a facile chemical method at room temperature. The characterizations of XPS, TEM, XRD and UV–vis spectra confirm that pure hexagonal wurtzite ZnO nanoparticles with an average size of about 9 nm are distributed on the surfaces of TNTs evenly and attached strongly. The photocatalytic activities of the ZnO–TNTs nanocomposite are superior to those of P25, ZnO, TNTs and ZnO–anatase TiO_2 (TNP) nanocomposite in the oxidation of rhodamine B under UV light irradiation. A comparison of the photocatalytic activities between different catalysts is discussed. Furthermore, we also find that the ZnO–TNT nanocomposite shows very favorable recycle use potential, because they have a high sedimentation rate and their photocatalytic activity is only slightly decreased even after five times of repeated uses.

1. Introduction

Recently, titanates with one-dimensional (1D) TiO_2 nanostructures such as nanotubes, nanowires and nanofibers [1–4] have attracted a lot of attention due to their significant potential applications. Among 1D titanate nanostructures, titanate nanotubes (TNTs), which are of layer structure with a hollow cavity, possess unique physicochemical properties and have become one of the most promising materials in various fields [5,6]. A great development has been achieved in the study of synthesis and the structure of these nanotubes [7–10]. In the past few years, increasing interests have being focused on the TNTs decorated with active catalysts, including metal ions and semiconductors in the application of catalysis process, such as photocatalysis, electrocatalysis and photoelectrocatalysis [11–13]. In fact, the high cation-exchange character as well as the particular tubular structure makes TNTs very suitable to act as the substrate and carrier for different catalysts that need to be immobilized. Furthermore, the decoration of enzymes [14], nanoparticles [15,16] and metal ion [17] with TNTs has resulted in better catalysis activities, because the unique physical properties of TNTs, such as open mesoporous morphology and high specific surface area, make the reagents easier to transport during the catalytic reaction [5]. All these interesting properties of TNTs encourage us to investigate it as a support for different catalysts.

Recently, ZnO becomes one of the most widely studied multifunctional nanocrystalline semiconductors and attracts attention for its wide range of applications, such as solar cells, luminescent, electrical and chemical sensors due to the wide band gap (3.2 eV) and large exciton binding energy (60 meV) [18–21]. The ZnO–TiO_2 nanoparticles have been synthesized successfully and the researches have proved that utilization of the nanocrystalline TiO_2 coupled with nanosized ZnO could improve their photocatalytic efficiency due to the synergistic effect on photocatalytic properties [22–25].

TNTs have several distinct advantages to be the substrate of ZnO–TNTs nanocomposite. Firstly, the high cation exchange properties make Zn^{2+} ions adsorb on TNTs more strongly and evenly [26]. Secondly, the surface area of TNTs, which include the inner-cavity and outer surface, is large enough to accommodate more ZnO nanoparticles [27]. Thirdly, TNTs are more convenient than spherical powder catalysts, such as P25, for separating catalysts from suspended solution because of the high sedimentation rate [28]. Some studies have shown the use of CdS–TNTs [29,30] or SnO_2–TNTs [31] nanocomposite can enhance the performance in photocatalysis. However, to the best of our knowledge, there are few reports regarding the properties of TNTs coupled with ZnO nanoparticles and their repeated use in photocatalysis. Herein, we report the preparation of ZnO–TNTs nanocomposite by a facile chemical method at room temperature. Their characterizations of XPS, TEM, XRD and UV–vis spectra are also discussed. The prepared nanocomposite show excellent photocatalytic properties on the degradation of rhodamine B (RhB) under UV irradiation. Further-

* Corresponding author. Tel.: +86 20 88586766; fax: +86 20 87112631.
E-mail address: wanglsh@scut.edu.cn (L.S. Wang).

0304-3894/$ – see front matter © 2008 Elsevier B.V. All rights reserved.
doi:10.1016/j.jhazmat.2008.03.080

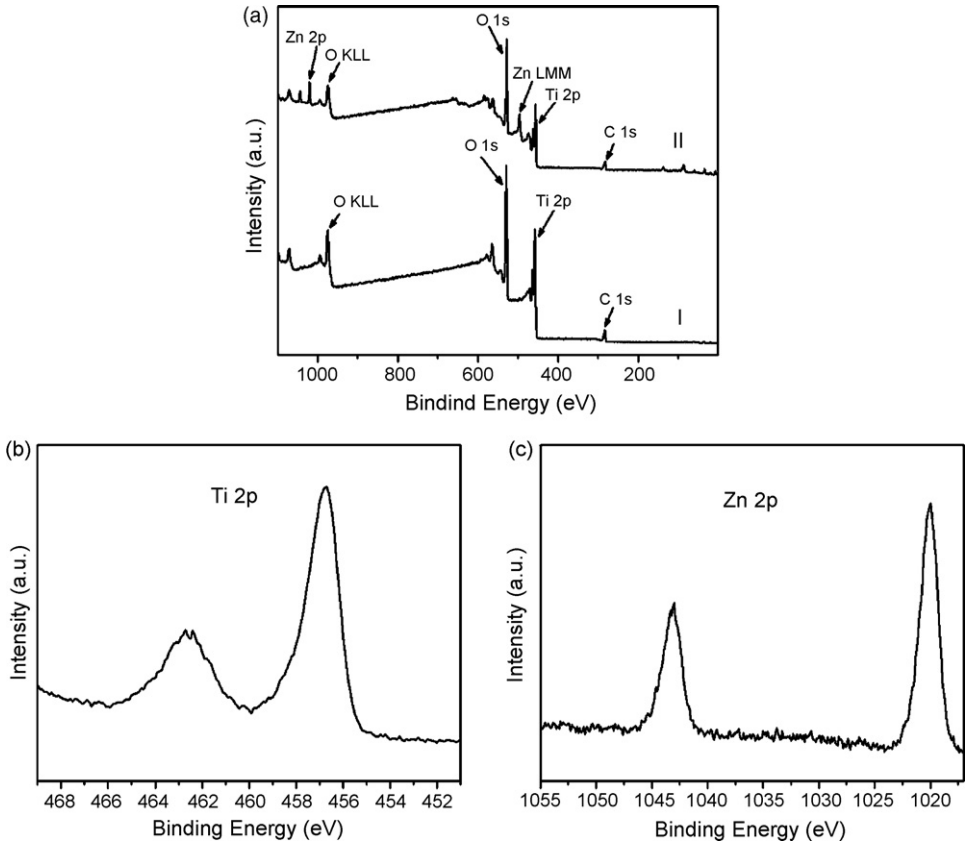

Fig. 1. (a) XPS survey spectra of TNTs (I) and ZnO–TNTs (II), (b) Ti 2p XPS spectra of ZnO(20 wt.%)–TNTs, (c) Zn 2p XPS spectra of ZnO(20 wt.%)–TNTs.

more, the recycle of ZnO–TNTs is more convenient and no obvious decrease in the photocatalytic activity is observed for the recycled ZnO–TNTs.

2. Experimental

2.1. Reagents and measurement

Zinc acetate, sodium hydroxide and RhB were of analytical reagent grade purchased from Guangzhou Chemical Reagents Factory (Guangzhou, China) and used without further purification. Deionized water was used in all aqueous solution preparations and washings.

2.2. Synthesis

2.2.1. Titanate nanotubes synthesis

TNTs were prepared following the literature procedure [32]. Briefly, 2 g of commercial anatase TiO_2 nanoparticles (TNP) was added to 50 mL of 10 M NaOH solution and heated for 24 h at 130 °C in a Teflon-lined autoclave. After cooled naturally in air, the mixture was centrifuged at a speed of 4000 rpm and the precipitates were collected. The white powder was thoroughly washed with water then with 0.1 M HCl, followed by vacuum drying at 70 °C.

2.2.2. Preparation of ZnO–TNTs nanocomposite

The ZnO–TNTs nanocomposite was synthesized by the following method. Stoichiometric amount of pure TNTs and zinc acetate was dispersed in 50 mL absolute ethanol by stirring for 6 h. Then the absolute ethanol solution of sodium hydroxide (50 mL, 0.2 M) was gradually added with vigorous stirring at room temperature. After the mixture was stirred for 10 h, a white precipitate was obtained. Then the white powder was collected by centrifugation and then washed several times with deionized water and ethanol for several times. In addition, the ZnO–TNP was prepared by using in a similar way in order to make a comparison of the photocatalytic properties with that of the ZnO–TNTs.

2.3. Characterizations

X-ray photoelectron spectroscopy (XPS) measurements were done with AXis Ultra^{DLD} (Kratos). The powder X-ray diffraction (XRD) patterns were recorded using an XD-3A Cu Kα X-ray diffrac-

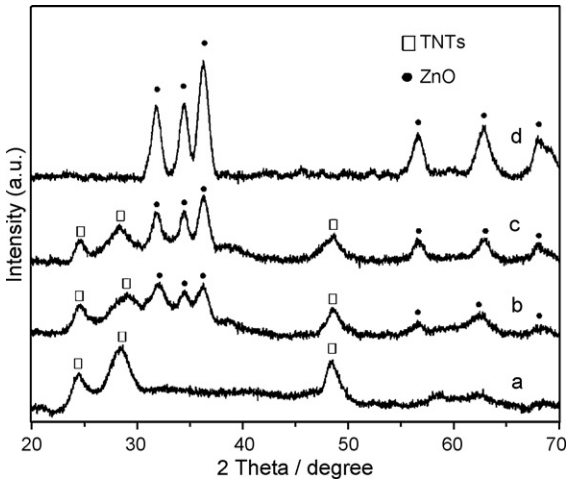

Fig. 2. X-ray diffraction patterns of (a) TNTs, (b) ZnO(10 wt.%)–TNTs, (c) ZnO(20 wt.%)–TNTs and (d) ZnO nanoparticles.

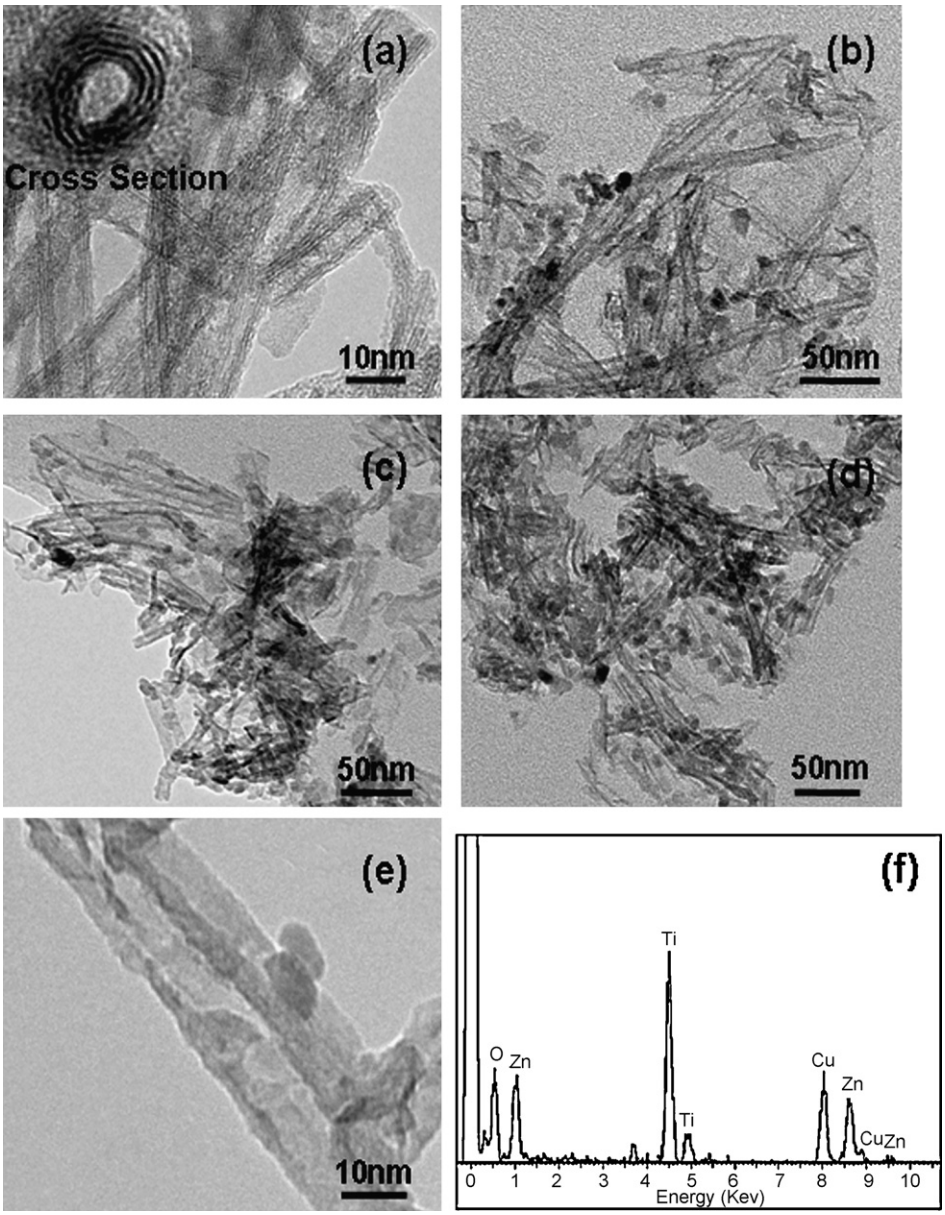

Fig. 3. TEM images of samples (a) as-prepared TNTs, (b) ZnO(10 wt.%)–TNTs nanocomposite, (c) ZnO(20 wt.%)–TNTs nanocomposite, (d) ZnO(30 wt.%)–TNTs nanocomposite, (e) high magnification images showing the single ZnO particle is supported on nanotubes and (f) EDX of ZnO(20 wt.%)–TNTs nanocomposite.

tometer (λ = 15.418 Å, Japan). Transmission electron microscope (TEM) measurement was conducted using a JEM-2010HR (JEOL Co. Ltd.). The UV–vis spectra were checked by a UV3100 spectrophotometer (Shimadzu Co., Kyoto, Japan).

2.4. Photocatalytic activity measurements

All the photocatalytic experiments were performed in 200 mL hollow cylindrical photoreactor equipment equipped with a glass water jacket (Prexy). A 300-W high-pressure mercury lamp was positioned in the inner part of the photoreactor and cooling water circulated through the water jacket surrounding the lamp. The average light intensity in the solution was about 8 mW cm^{-2}. Batch experiments were conducted at 30 °C. In a typical reaction, 150 mL of 12 mg L^{-1} RhB solution and 200 mg photocatalysts was added in reactor under the magnetic stirring for 15 min in dark firstly and then the mercury lamp was turned on. At regular irradiation time intervals, the dispersion was sampled (3 mL) and centrifuged to separate the samples. The residual RhB concentration was detected by UV–vis. For cycling use experiments, after the ZnO–TNTs nanocomposite were separated from suspended solution by sedimentation for 1 h, we removed the upper clear solution, and then the ZnO–TNTs nanocomposite were dispersed in 150 mL RhB aqueous solution for another cycling use.

3. Results and discussion

3.1. Characterizations of ZnO–TNTs nanocomposite

3.1.1. XPS analysis

XPS measurements were performed to determine the chemical composition of the prepared samples and the valence states of various species. Fig. 1a shows the XPS survey spectra of pure TNTs and ZnO–TNTs nanocomposite. It can be seen that the obvious peaks

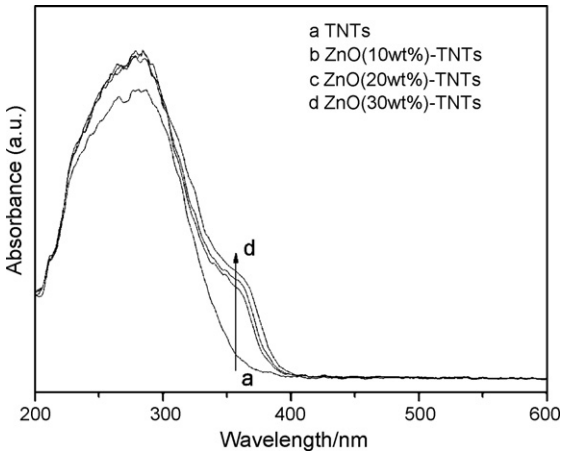

Fig. 4. UV–vis spectra of (a) TNTs and ZnO–TNTs nanocomposite with different ZnO concentrations (b) 10 wt.%, (c) 20 wt.% and (d) 30 wt.%.

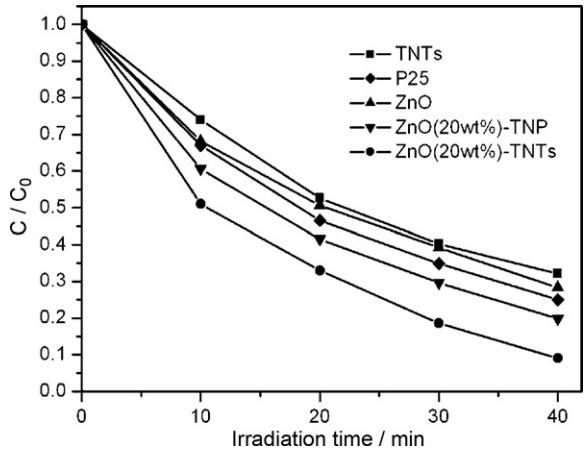

Fig. 5. Effect of illumination time on the degradation of RhB when using different catalysts.

mainly attribute to the Ti, O and C element. For the TNTs coated with ZnO, the additional peaks of the Zn 2p appear in the survey spectra of the ZnO–TNTs nanocomposite. These XPS spectra can serve as an evidence for the formation of ZnO–TNTs nanocomposite and indicate that the nanocomposite contain not only Ti, O and C elements but also Zn element, which is the component of ZnO molecules. The high-resolution XPS spectra in Fig. 1b and c shows the characteristic peaks of Ti 2p and Zn 2p of ZnO–TNTs nanocomposite. The binding energy peaks located at 1021.3 and 1044.1 eV are attribute to the spin–orbit splitting of the Zn 2p components, which are in good agreement with those of zinc oxide powder (Fig. 1c) [33]. Similarly, the peaks located at 456.8 and 462.6 eV are attribute to the spin–orbit splitting of the Ti 2p components, which are in good agreement with the titanium(IV) species (Fig. 1b) [34]. Therefore, it is evident that the zinc and titanium in the nanocomposite are present in the 2-valent state and 4-valent state, respectively.

3.1.2. XRD analysis and TEM images

The XRD profile for TNTs, ZnO(10 wt.%)–TNTs, ZnO(20 wt.%)–TNTs and pure ZnO samples are displayed in Fig. 2 We can observe that the characteristic XRD patterns for TNTs and ZnO crystallites are visible in the nanocomposite. The obvious peaks of TNTs are found at 24.4°, 28.2° and 48.2° corresponding to (1 1 0), (3 1 0) and (0 2 0) crystal planes, respectively [35–38]. Meanwhile, there are additional peaks at angles (2θ) of 31.7°, 34.4°, 36.2°, 56.5°, 62.8° and 67.5°, which could be assigned to the ZnO phase (1 0 0), (0 0 2), (1 0 1), (1 1 0), (1 0 3) and (1 1 2) crystal planes, respectively (JCPDS 36-1451) [39,40]. This reveals that the resultant nanoparticles formed on TNTs are the hexagonal ZnO nanoparticles with a wurtzite structure. According to the Scherrer's formula, the average size of the ZnO particles in TNTs is estimated to be about 9 nm.

Fig. 3 shows the TEM images of the as-prepared TNTs and ZnO–TNTs nanocomposite coated with different amounts of ZnO. The typical morphologies of the as-prepared TNTs are displayed in Fig. 3a. The TEM images show that the TNTs present uniform distribution in an average diameter of 10 nm with a layered structure, and the hollow nature of tubes opening on both ends can also be observed clearly. A single nanotube is multi-layed wall with an inter shell spacing of 0.8 nm and 5–6 nm in the inner diameter. The morphologies of TNTs change greatly after TNTs are decorated with ZnO particles. Fig. 3b–d shows the representative TEM images of the nanotubes after the decoration with different concentration of ZnO nanoparticles. It can be seen that most of the nanosized ZnO nanoparticles are distributed on the surfaces of TNTs evenly and densely and only a small amount of ZnO are encapsulated in the cavity of TNTs. In addition, the amount of ZnO nanoparticles formed on TNTs varies and more ZnO nanoparticles surround the surface of TNTs with the increase of Zn^{2+} ions concentration. These images indicate that the morphology of ZnO–TNTs nanocomposite can be changed by adjusting the concentrations of the precursors. Fig. 3e depicts an HRTEM image demonstrating that the ZnO nanoparticles are adsorbed on the walls of TNTs and the ZnO nanocrystals have dimensions of about 9 nm, which is consistent with the analysis of XRD data. The EDX in Fig. 3f confirm the elemental composition of Zn and also show the signals of copper, titanium and oxygen originated from copper grid and TNTs.

3.1.3. UV–vis diffuse reflection spectroscopy

The UV–vis diffuse reflection spectra of TNTs, ZnO(10 wt.%)–TNTs, ZnO(20 wt.%)–TNTs and ZnO(30 wt.%)–TNTs samples are present in Fig. 4. As shown in Fig. 4, the maximum adsorption wavelengths of TNTs and ZnO(10 wt.%)–TNTs are 360 and 385 nm, indicating an obvious red shift of ZnO–TNTs composite compared with TNTs. In addition, it also has been found that the slight red shift occurs with the increase of the concentration of ZnO decorated on TNT. It has been reported that wavelength of the absorption edge of ZnO and TiO_2 was 391 and 365 nm, respectively [41]. Therefore, the light absorption scope of ZnO–TNTs nanocomposite is enlarged when compared with TNTs due to the existence of ZnO that modifies the optical absorption edge.

3.2. Photocatalytic activity of ZnO–TNTs nanocomposite

The kinetic curves of the photocatalytic RhB degradation with different catalysts in the presence of O_2 through magnetic stirring are shown in Fig. 5. Compared with the pure TNTs, P25 and ZnO photocatalysts, enhanced photocatalytic properties of the ZnO–TNTs nanocomposite can be observed as expected. The results of higher photocatalytic activity are primarily attributed to the coupling effect of TNTs and ZnO particles. Fig. 6 shows the mechanistic scheme of the charge separation and photocatalytic reaction for ZnO–TNTs photocatalysts [42–44]. As illustrated in this scheme, the photo-generated electrons inject into the conduction band of TNTs from that of the excited ZnO nanoparticles. On the other hand, the transfer of photo-generated hole also occurs from the valence band of TNTs to that of ZnO similarly. Such an efficient charge separation increases the lifetime of the charge carriers and enhances the efficiency of the interfacial charge transfer to adsorbed substrates. Thus, the photocatalytic properties increase because the possibilities of recombination between photo-generated electron and hole

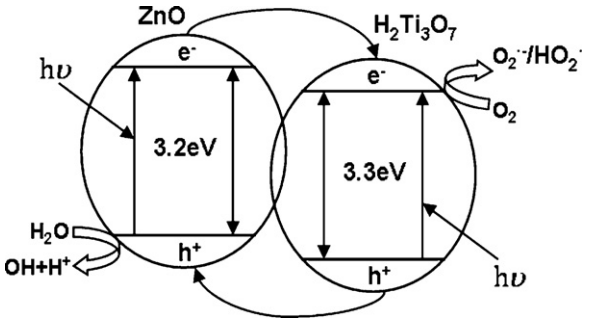

Fig. 6. A schematic diagram illustrating the principle of charge separation and photocatalytic activity for the ZnO–TNTs system.

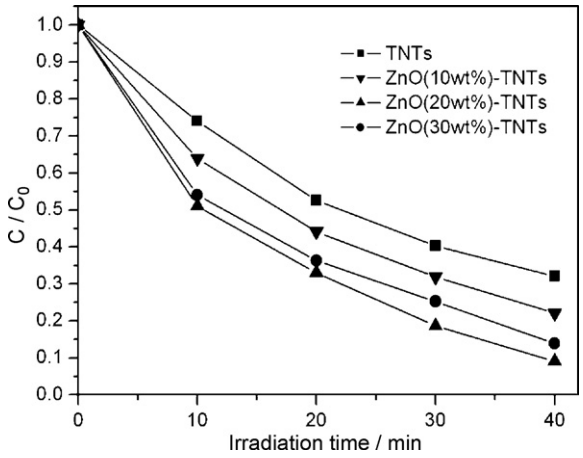

Fig. 7. Photocatalytic activity of ZnO–TNTs nanocomposite with different ZnO content.

are reduced through facilitating their separation. In addition, we also find that the photocatalytic activity of ZnO–TNTs is higher than ZnO–TNP with the same fraction of ZnO in RhB degradation according to Fig. 5. Compared with ZnO–TNP, it indicated that the larger surface area as well as the unique tubular structure of TNTs might facilitate the moving of photo-produced electron and the contact of organic molecules, which are both beneficial for the degradation reaction [45].

Fig. 7 shows that the photocatalytic activity of ZnO–TNTs nanocomposite is related to the content of ZnO coated on TNTs.

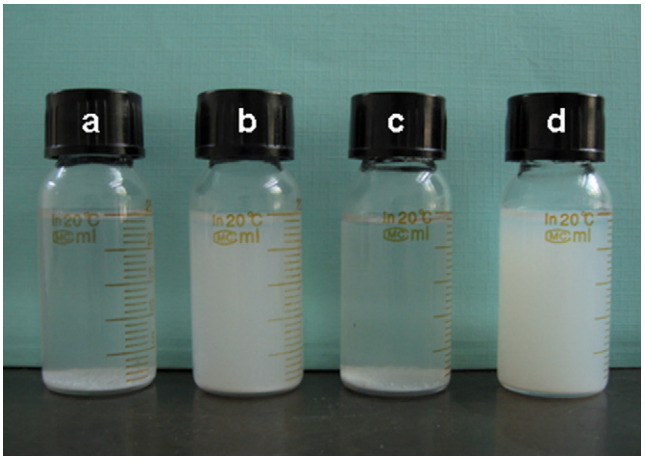

Fig. 8. Sedimentation for 1 h in aqueous suspensions of (a) ZnO (20 wt.%)–TNTs, (b) TNP, (c) TNTs and (d) P25 (concentration: 0.5 g/L, ultrasonic treatment for 15 min).

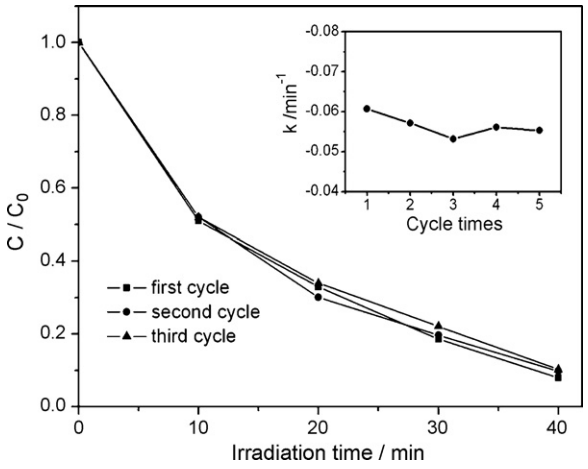

Fig. 9. Photocatalytic activity of the ZnO(20 wt.%)–TNTs nanocomposite for RhB degradation with three times of cycling uses. Inset: overall degradation rate constant *k* vs. times of cycling uses for RhB degradation of ZnO(20 wt.%)–TNTs photocatalysts.

When the proportion of ZnO is low (10 wt.%), the effect of charge separation induced by ZnO is not obvious because of the insufficiency of ZnO. However, when the concentration of ZnO increases to 30 wt.%, quite a number of ZnO nanoparticles would surround some active sites of TNTs and hinder the contact between TNTs and oxygen contained species, which result in the decrease of photocatalytic properties. According to Fig. 7, the ZnO(20 wt.%)–TNTs nanocomposite is considered as the optimal ZnO content among the prepared nanocomposite at different quantity of ZnO nanoparticles.

As well known, the spherical catalysts powders with small size present a superior activity due to the large surface-to-volume ratios. However, in a particular photocatalytic process, the separation of these powdered photocatalysts from suspended solution after reaction could be very difficult for the recycle use. The photocatalysts of titanate nanotubes have taken an advantage over spherical powder catalysts for separating catalysts by sedimentation [46]. In our experiment, one of the advantages of ZnO–TNTs is that they may be conveniently separated to recycle the catalysts. According to Fig. 8, the TNTs and ZnO–TNTs nanocomposite sedimentated from an aqueous suspension in 1 h, while the aqueous suspension of P25 and TNP is still relatively turbid. In addition, the catalytic activity of the repeated ZnO–TNTs nanocomposite is also studied. As shown in Fig. 9, after a five-time recycling of ZnO–TNTs nanocomposite, there is still appreciable degradation of RhB in the aqueous solution upon irradiation. In fact, the rate constant in the photocatalytic activity for the repetitive uses of the same ZnO–TNTs photocatalysts has no obvious reduction.

4. Conclusion

In summary, the ZnO–TNTs nanocomposites with different amount of ZnO have been synthesized by a simple chemical method at room temperature. The obtained ZnO–TNTs nanocomposite is characterized by different methods, including XPS, TEM, XRD and UV–vis absorption measurements. As expected, the ZnO–TNTs nanocomposite exhibits higher activity for photodegradation of RhB than pure TNTs, P25 and ZnO. Furthermore, the ZnO–TNTs nonocomposites are also easy to recycle for photocatalytic purpose in that their activity remains similar after five repeated cycles. The ZnO–TNTs nanocomposite with the properties of higher photocatalytic activity and easier separation for recycle use show promising prospect as photocatalysts for the degradation of organic pollutant from water in future industrial application.

Acknowledgments

This work is supported by the National Natural Science Foundation of China (No. 20475018) and the Nature Science Foundation of Guangdong (No. 07006544).

References

[1] H. Tokudome, M. Miyauchi, Electrochromism of titanate-based nanotubes, Angew. Chem. Int. Ed. 44 (2005) 1974–1977.
[2] Y. Lan, X.P. Gao, H.Y. Zhu, Z.F. Zheng, T.Y. Yan, F. Wu, S.P. Ringer, D.Y. Song, Titanate nanotubes and nanorods prepared from rutile powder, Adv. Funct. Mater. 15 (2005) 1310–1318.
[3] A.R. Armstrong, G. Armstrong, J. Canales, P.G. Bruce, TiO_2–B nanowires, Angew. Chem. Int. Ed. 43 (2004) 2286–2288.
[4] H.Y. Zhu, X.P. Gao, Y. Lan, D.Y. Song, Y.X. Xi, J.C. Zhao, Hydrogen titanate nanofibers covered with anatase nanocrystals: a delicate structure achieved by the wet chemistry reaction of the titanate nanofibers, J. Am. Chem. Soc. 126 (2004) 8380–8381.
[5] D.V. Bavykin, J.M. Friedrich, F.C. Walsh, Protonated titanates and tio$_2$ nanostructured materials synthesis, properties, and applications, Adv. Mater. 18 (2006) 2807–2824.
[6] A. Thorne, A. Kruth, D. Tunstall, J.T.S. Irvine, W.Z. Zhou, Formation, structure, and stability of titanate nanotubes and their proton conductivity, J. Phys. Chem. B 109 (2005) 5439–5444.
[7] X.M. Sun, X. Chen, Y.D. Li, Large-scale synthesis of sodium and potassium titanate nanobelts, Inorg. Chem. 41 (2002) 4996–4998.
[8] B.D. Yao, Y.F. Chan, X.Y. Zhang, W.F. Zhang, Z.Y. Yang, N. Wang, Formation mechanism of TiO_2 nanotubes, Appl. Phys. Lett. 82 (2003) 281–283.
[9] R. Ma, Y. Bando, T. Sasaki, Nanotubes of lepidocrocite titanates, Chem. Phys. Lett. 380 (2003) 577–582.
[10] S. Zhang, L.M. Peng, Q. Chen, G.H. Du, G. Dawson, W.Z. Zhou, Formation mechanism of $H_2Ti_3O_7$ nanotubes, Phys. Rev. Lett. 91 (2003) 256103.
[11] J.R. Li, Z.L. Tang, Z.T. Zhang, H-titanate nanotube novel lithium intercalation host with large capacity and high rate capability, Electrochem. Commun. 7 (2005) 62–67.
[12] D.V. Bavykin, A.A. Lapkin, P.K. Plucinski, L.T. Murciano, J.M. Friedrich, F.C. Walsh, Deposition of Pt, Pd, Ru and Au on the surfaces of titanate nanotubes, Top. Catal. 39 (2006) 151–159.
[13] A. Ghicov, H. Tsuchiya, J.M. Macak, P. Schmuki, Annealing effects on the photoresponse of TiO_2 nanotube, Phys. Stat. Sol. 203 (2006) R28–R30.
[14] J.P. Qu, X.G. Zhang, Y.G. Wang, C.G. Xie, Electrochemical reduction of CO_2 on RuO_2/TiO_2 nanotubes composite modified Pt electrode, Electrochim. Acta 50 (2005) 3576–3580.
[15] L.T. Murciano, A.A. Lapkin, D.V. Bavykin, F.C. Walsh, K. Wilson, Highly selective Pt/titanate nanotube catalysts for the double-bond migration reaction, J. Catal. 245 (2007) 272–278.
[16] V. Idakiev, Z.Y. Yuan, T. Tabakova, B.L. Su, Titanium oxide nanotubes as supports of nano-sized gold catalysts for low temperature water–gas shift reaction, Appl. Catal. A 281 (2005) 149–155.
[17] T. Akita, M. Okumura, K. Tanaka, K. Ohkuma, M. Kohyama, T. Koyanagi, M. Date, S. Tsubota, M. Haruta, Transmission electron microscopy observation of the structure of TiO_2 nanotube and Au/TiO_2 nanotube catalyst, Surf. Interf. Anal. 37 (2005) 265–269.
[18] H. Zhang, D.R. Yang, X.Y. Ma, Y.J. Ji, J. Xu, D.L. Que, Synthesis of flower-like ZnO nanostructures by an organic-free hydrothermal process, Nanotechnology 15 (2004) 622–626.
[19] P.D. Yang, H.Q. Yan, S. Mao, R. Russo, J. Johnson, R. Saykally, N. Morris, J. Pham, R.R. He, H.J. Choi, Controlled growth of ZnO nanowires and their optical properties, Adv. Funct. Mater. 12 (2002) 323–331.
[20] H. Kind, H.Q. Yan, B. Messer, M. Law, P.D. Yang, Nanowire ultraviolet photodetectors and optical switches, Adv. Mater. 14 (2002) 158–160.
[21] T. Gao, Q.H. Li, T.H. Wang, Sonochemical synthesis, optical properties, and electrical properties of core/shell-type ZnO nanorod/CdS nanoparticle composites, Chem. Mater. 17 (2005) 887–892.
[22] V. Sukharev, R. Kershaw, Concerning the role of oxygen in photocatalytic decomposition of salicylic acid in water, J. Photochem. Photobiol. A 98 (1996) 165–169.
[23] N. Serpone, P. Maruthamuthu, P. Pichat, E. Pelizzetti, H. Hidaka, Exploiting the interparticle electron transfer process in the photocatalyzed oxidation of phenol, 2-chlorophenol and pentachlorophenol: chemical evidence for electron and hole transfer between coupled semiconductors, J. Photochem. Photobiol. A 85 (1995) 247–255.
[24] X. Fu, L.A. Clark, Q. Yang, M.A. Anderson, Enhanced photocatalytic performance of titania-based binary metal oxides: TiO_2/SiO_2 and TiO_2/ZrO_2, Environ. Sci. Technol. 30 (1996) 647–653.
[25] S.G. Yang, Q. Xie, X.Y. Li, Y.Z. Liu, S. Chen, G.H. Chen, Preparation, characterization and photoelectrocatalytic properties of nanocrystalline Fe_2O_3/TiO_2, ZnO/TiO_2, and Fe_2O_3/ZnO/TiO_2 composite film electrodes towards pentachlorophenol degradation, Phys. Chem. Chem. Phys. 6 (2004) 659–664.
[26] X.M. Sun, Y.D. Li, Synthesis and characterization of ion-exchangeable titanate nanotubes, Chem. Eur. J. 9 (2003) 2229–2238.
[27] D.V. Bavykin, E.V. Milsom, F. Marken, D.H. Kim, D.H. Marsh, D.J. Riley, F.C. Walsh, K.H. El-Abiary, A.A. Lapkin, A novel cation-binding TiO_2 nanotube substrate for electro- and bioelectro-catalysis, Electrochem. Commun. 7 (2005) 1050–1058.
[28] Y.X. Yu, D.S. Xu, Single-crystalline TiO_2 nanorods: highly active and easily recycled photocatalysts, Appl. Catal. B 73 (2007) 166–171.
[29] M. Hodos, E. Horváth, H. Haspel, Á. Kukovecz, Z. Kónya, I. Kiricsi, Photosensitization of ion-exchangeable titanate nanotubes by CdS nanoparticles, Chem. Phys. Lett. 399 (2004) 512–515.
[30] H. Li, B.L. Zhu, Y.F. Feng, S.R. Wang, S.M. Zhang, W.P. Huang, Synthesis, characterization of TiO_2 nanotubes-supported MS (TiO_2NTs@MS, M = Cd, Zn) and their photocatalytic activity, J. Solid State Chem. 180 (2007) 2136–2142.
[31] L.R. Hou, C.Z. Yuan, Y.P. Peng, Synthesis and photocatalytic property of SnO_2/TiO_2 nanotubes composites, J. Hazard. Mater 139 (2007) 310–315.
[32] T. Kasuga, M. Hiramatsu, A. Hoson, T. Sekino, K. Niihara, Formation of titanium oxide nanotube, Langmuir 14 (1998) 3160–3163.
[33] S.S. Kim, J.H. Yum, Y.E. Sung, Flexible dye-sensitized solar cells using ZnO coated TiO_2 nanoparticles, J. Photochem. Photobiol. A 171 (2005) 269–273.
[34] C. Huang, X. Liu, L. Kong, W. Lan, Q. Su, Y. Wang, The structural and magnetic properties of Co-doped titanate nanotubes synthesized under hydrothermal conditions, Appl. Phys. A 87 (2007) 781–786.
[35] C.C. Tsai, H.S. Teng, Structural features of nanotubes synthesized from NaOH treatment on TiO_2 with different post-treatments, Chem. Mater. 18 (2006) 367–373.
[36] D.V. Bavykin, V.N. Parmon, A.A. Lapkin, F.C. Walsh, The effect of hydrothermal conditions on the mesoporous structure of TiO_2 nanotubes, J. Mater. Chem. 14 (2004) 3370–3377.
[37] Q. Chen, W.Z. Zhou, G.H. Du, L.M. Peng, Trititanate nanotubes made via a single alkali treatment, Adv. Mater. 14 (2002) 1208–1211.
[38] J.J. Yang, Z.S. Jin, X.D. Wang, W. Li, J.W. Zhang, S.N. Zhang, X.Y. Yong, Z.J. Zhang, Study on composition, structure and formation process of nanotube $Na_2Ti_2O_4(OH)_2$, Dalton Trans. 20 (2003) 3898–3901.
[39] C.L. Wu, X.L. Qiao, J.G. Chen, H.S. Wang, F.T. Tan, S.T. Li, A novel chemical route to prepare ZnO nanoparticles, Mater. Lett. 60 (2006) 1828–1832.
[40] X.P. Gao, Z.F. Zheng, H.Y. Zhu, G.L. Pan, J.L. Bao, F. Wu, D.Y. Song, Rotor-like ZnO by epitaxial growth under hydrothermal conditions, Chem. Commun. 12 (2004) 1428–1429.
[41] W. Wu, Y.W. Cai, J.F. Chen, S.L. Shen, A. Martin, L.X. Wen, Preparation and properties of composite particles made by nanozinc oxide coated with titanium dioxide, J. Mater. Sci. 41 (2006) 5845–5850.
[42] D.L. Liao, C.A. Badour, B.Q. Liao, Preparation of nanosized TiO2/ZnO composite catalyst and its photocatalytic activity for degradation of methyl orange, J. Photochem. Photobiol. A 194 (2008) 11–19.
[43] D. Robert, Photosensitization of TiO_2 by M_xO_y and M_xS_y nanoparticles for heterogeneous photocatalysis applications, Catal. Today 122 (2007) 20–26.
[44] M.W. Xiao, L.S. Wang, Y.D. Wu, X.J. Huang, Z. Dang, Preparation and characterization of CdS nanoparticles decorated into titanate nanotubes and their photocatalytic properties, Nanotechnology 19 (2008) 015706.
[45] J.C. Xu, M. Lu, X.Y. Guo, H.L. Li, Zinc ions surface-doped titanium dioxide nanotubes and its photocatalysis activity for degradation of methyl orange in water, J. Mol. Catal. 226 (2005) 123–127.
[46] H.Y. Zhu, Y. Lan, X.P. Gao, S.P. Ringer, Z.F. Zheng, D.Y. Song, J.C. Zhao, Phase transition between nanostructures of titanate and titanium dioxides via simple wet-chemical reactions, J. Am. Chem. Soc. 127 (2005) 6730–6736.